PRINTED WIDE-SLOT ANTENNA WITH HIGH POLARIZATION PURITY FOR WIDEBAND APPLICATIONS

Mohammad Naser-Moghadasi,[1] Reza Bayderkhani,[2] Gholamreza Dadashzadeh,[3] and Bal S. Virdee[3]
[1] Faculty of Engineering, Science and Research Campus, Islamic Azad University, Tehran, Iran; Corresponding author: mn.moghaddasi@srbiau.ac.ir
[2] Department of Electrical Engineering, Faculty of Engineering, Shahed University, Tehran, Iran
[3] Faculty of Computing, London Metropolitan University, 166-220 Holloway Road, London N7 8DB, United Kingdom

Received 8 July 2009

ABSTRACT: *This article describes a novel compact wideband slot antenna comprising of an E-shaped patch that is excited with a trident-shaped microstrip feed-line structure. The antenna design exhibits a very wide operating bandwidth of over 163% with* $S_{11} < -10$ *dB in the frequency range 2–19.95 GHz. The antenna's radiation characteristics are stable across the 2–12 GHz band. The proposed antenna exhibits high polarization purity with cross-polarization level that is well below −50 dB. A comprehensive parametric study was performed on the antenna to fully understand the effects of various antenna parameters that enable optimization of the antenna's performance. This antenna easily fulfills the requirements for ultra-wideband wireless communication systems as specified by federal communication commission over the designated band 3.1–10.6 GHz.* © 2010 Wiley Periodicals, Inc. Microwave Opt Technol Lett 52: 1001–1006, 2010; Published online in Wiley InterScience (www.interscience.wiley.com). DOI 10.1002/mop.25096

Key words: *slot antenna; ultra-wideband; microstrip feed*

1. INTRODUCTION

Ultra-wideband (UWB) antennas for wireless communication applications have gained a great deal of attention and impetus recently after the federal communication commission (FCC) approved the commercial use of 3.1–10.6 GHz band [1]. UWB communication systems will offer enormous available bandwidth permitting high-speed data transmission of 500 M/bps to 1 G/bps to be achieved. As is the case for conventional wireless communication systems, antennas will play a very crucial role in UWB systems. However, the design of UWB antennas presents a significantly more challenge than is the case for narrow band antennas. A suitable UWB antenna should be capable of operating over the entire ultra-wide bandwidth allocated by the FCC. Concurrently, the antenna needs to satisfy omnidirectional radiation coverage over the specified frequency range.

Planar monopole and printed wide-slot antennas are the good candidates for use in UWB wireless technology because of their relatively wide impedance bandwidth and approximately omnidirectional azimuthal radiation patterns. However, the planar monopole, which is a metallic configuration, is not the most preferred option for UWB application because it is generally mounted on a large ground plane, which is perpendicular to the plane of monopole. This feature is undesirable as it makes the antenna a 3D structure. Furthermore, the large size of the ground plane limits the antenna's radiation pattern to only one half hemisphere. However, printed wide-slot antenna is a truly planar structure, which has radiation patterns comparable to that of a dipole antenna.

Printed wide-slot microstrip antennas have numerous attractive features, namely, small size, light weight, low cost, ease of fabrication, and integration with planar and nonplanar surfaces. These features make this type of antenna widely used in a variety of communication systems [2–6]. It is also well known that wide-slot antenna acts more similar to a printed monopole antenna, especially when the size of the slot is large. The disadvantage of this type of antenna is that its bandwidth is narrow. In an attempt to simplify the antenna's structure, it is fed using a CPW instead of a microstrip line; however, this has a detrimental impact on its impedance bandwidth, which is further reduced [7]. Some bandwidth enhancement techniques using the CPW-fed slot antennas have resulted in some impedance bandwidth improvement, but it is limited to about 60% [8].

To enhance the bandwidth of a patch antenna, several approaches have been proposed previously, such as using a thick substrate with low dielectric constant and multiple resonators [9], parasitic patches stacked on the top of the main patch or close to main patch in the same plane [10], U-shaped slot [11], L-probe feeding [12], lossy materials [13], a capacitively probe fed structure [14], and a 3D transition microstrip feed-line [15].

Significant effort has been made to determine the planar shape, which provides the widest input bandwidth, but very little effort to date has been directed on understanding the physical behavior on the antenna's performance. In [16], the theory of characteristic modes introduced by Harrington and Mautz [17] is used to analyze the eigenmodes of the various shaped printed monopole antennas.

In this article, a unique technique is introduced to overcome the impedance bandwidth limitation associated with wide-slot antenna. The proposed wideband slot antenna is excited by an E-shaped patch, which is fed with microstrip line in the form of a trident shape. To acquire insight of antenna's performance, its current distribution is studied. The proposed antenna configuration is small in size and has a substantially wider bandwidth compared with an equivalent wide-slot antenna in [2]. An impedance bandwidth achieved for the antenna proposed in this article is over 163% from 2 to 19.95 GHz with $S_{11} < -10$ dB. In addition, this configuration provides high polarization purity. The proposed printed wide-slot antenna was analyzed with a commercially available full-wave finite element electromagnetic (EM) simulator.

2. ANTENNA DESIGN AND STRUCTURE

Characteristic modes (J_n) are real current modes that are excited on the antenna's surface. These modes are generally extracted at every frequency of interest to determine the antenna's property [17]. In [16], the characteristic modes of various shapes of the printed monopole antennas are investigated. The computational results show that when a center feed stripline is used then only vertical current modes (J_1 and J_3) are excited. However, any changes in position of the feed-line will result in the excitation of transverse modes, like mode J_2, which can deteriorate the antenna's polarization purity. This mechanism is exploited in this article to modify the shape of the patch antenna and its feed-line network to realize an antenna with ultra-wide bandwidth characteristic exhibiting high polarization purity. In the next sections, details of how these modifications affect the performance of the proposed antenna are presented.

Figures 1(a) and 1(b) show the proposed wide-slot antenna fed by microstrip line. This antenna was fabricated on a dielectric substrate with thickness of 1 mm and relative permittivity of $\varepsilon_r = 2.33$. The proposed antenna uses E-shaped patch with a trident-shaped feed-line structure to excite the slot on the ground plane. As will be shown later, this configuration provides a very wide impedance bandwidth and good radiation patterns. The substrate size is 70 mm × 80 mm. The dimensions of the proposed antenna are as follows: $L_s = 26$ mm, $W_s = 42$ mm, $L_p =$

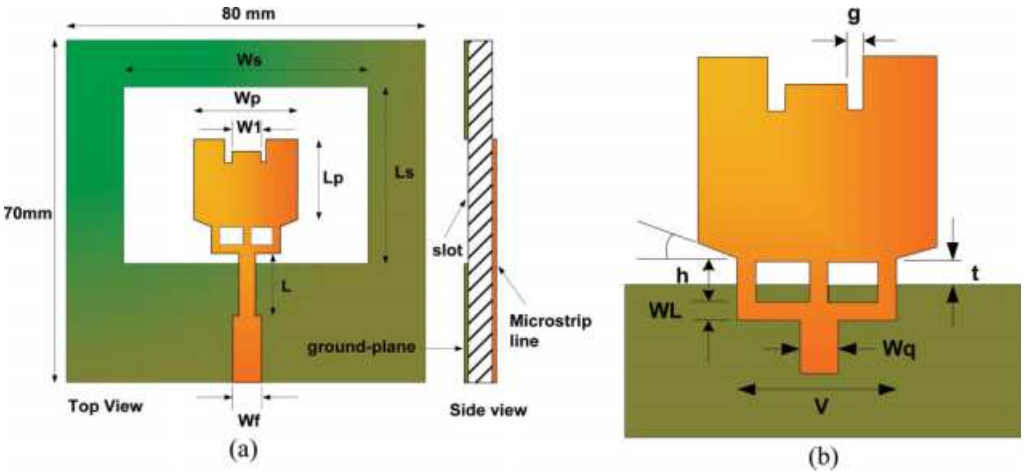

Figure 1 (a) Structure of the proposed wide-slot antenna fed with a microstrip line (top and side views). (b) Feeding structure of the proposed wide-slot antenna. [Color figure can be viewed in the online issue, which is available at www.interscience.wiley.com]

11 mm, $W_p = 14$ mm, $W_1 = 4$ mm, $g = 1$ mm, $L = 12$ mm, $W_f = 2.3$ mm, $\theta = 15°$, $h = 1.7$ mm, $W_L = 0.8$ mm, $t = 1$ mm, $V = 9.3$ mm, and $W_q = 1.7$ mm.

3. RESULTS AND DISCUSSION

In this section, the simulation and experimental results of the wide-slot antenna design are presented and discussed. All simulations were done using Ansoft's HFSS, which is based on the finite element. Also, to validate the simulation results, the antenna design was fabricated and tested. Figures 2(a) and 2(b) show the surface current distribution on the patch at 3 and 7 GHz, respectively. The current distribution at these frequencies is over the majority of patch's surface with current concentrations located in the vicinity of the outer feed-lines, thus representing the fundamental mode. At these frequencies, the current null is limited at the upper regions of the E-shape patch. At higher frequencies, for example, 10 and 13 GHz, the current distribution has more half-cycle variations resulting in current nulls at the patch's center and intense current regions at outer edges and near the outer feed-lines, as shown in Figures 2(c) and 2(d). It is observed in the simulations that the current null migrates toward the top of the patch as the frequency increases. This is indicative of higher order mode generation. These results agree well with those obtained using the theory of characteristics modes in [16].

The simulated and measured reflection coefficient of the optimized proposed antenna is shown in Figure 3. The results show the antenna provides a very wide impedance bandwidth of over 163% from a frequency of 2 to 19.95 GHz for which $S_{11} < -10$ dB. Compared with the antenna proposed in [2], the impedance bandwidth is significantly wider by more than 12.5 GHz. Detailed numerical and experimental investigation confirms that the impedance bandwidth is limited by the impedance match between the feed-line shape, in particular number of feed branches, and the ground plane wide-slot.

To understand the effect of the feed branches on the impedance bandwidth of proposed antenna, three types of antennas are studied. Antenna-1 has a single feed-line structure, antenna-2 has a dual feed-line, and antenna-3 has a trident-shaped feed-line, as it is depicted in Figure 4. This figure shows the distribution of the current vectors over the E-shaped patch using the different feed-line structures. The trident-shaped feed-line provides current vectors aligned upward in one direction, which indicates that high polarization is achieved with this structure.

The reflection coefficient of the three antennas 1, 2, and 3 is shown in Figure 5. This simulated result shows that the

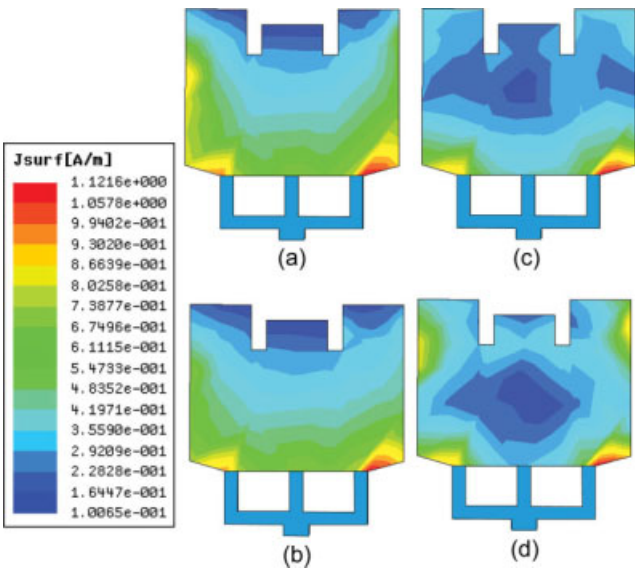

Figure 2 Current distribution on the patch at: (a) 3 GHz, (b) 7 GHz, (c) 10 GHz, and (d) 13 GHz. [Color figure can be viewed in the online issue, which is available at www.interscience.wiley.com]

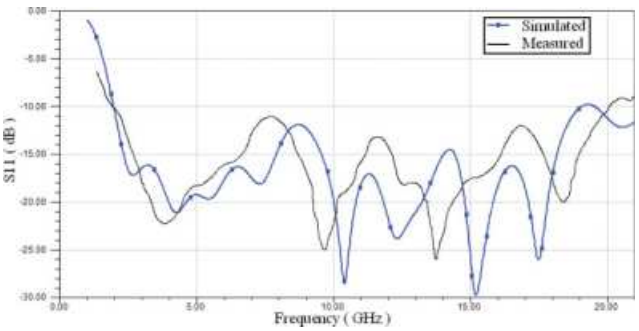

Figure 3 The simulated and measured reflection coefficient response of the proposed antenna. [Color figure can be viewed in the online issue, which is available at www.interscience.wiley.com]

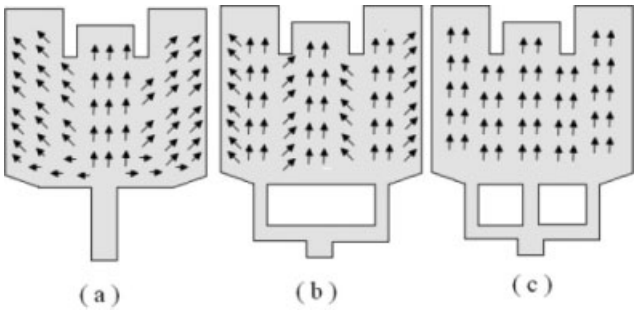

Figure 4 Current distribution vectors over the antenna patch using different feed-lines: (a) single feed, (b) double feed, and (c) trident-shaped feed

antenna's bandwidth can be enhanced by multiplying the feed-line access to the patch. Bandwidth enhancement is due to the vertical electrical current alignment in the proposed patch, as shown in Figure 4, which results in a uniform distribution of the magnetic current within the slot. Therefore, this confirms that by having a multiple feed-line to the patch eliminates the horizontal electrical current in the patch that results in the improvement of the antenna's cross-polarization characteristic.

The proposed antenna's simulated and measured copolar and cross-polar far-field *E*-plane (*y*–*z* plane) and *H*-plane (*x*–*z* plane) radiation patterns at 3, 7, and 11 GHz are shown in Figure 6. This figure shows that the antenna has good radiation patterns and relatively low cross-polarization in the band 2–12 GHz. The copolar/cross-polar ratio of better than 50 dB is observed at boresight in all of the measured radiation patterns. The cross-polarization levels at other directions are very low, indicating excellent polarization purity. As is evident from Figure 6, the proposed antenna provides symmetrical radiation patterns. At the higher frequency the radiation pattern is marginally distorted because of the unequal phase distribution of electrical fields on the slot and increased magnitudes of higher order modes. From this figure, it can be seen that the simulation results are in good agreement with the experimental results. The radiation bandwidth (2–12 GHz) of the proposed antenna easily accommodates the requirements for UWB wireless communications systems with bandwidth between 3.1 and 10.6 GHz.

The measured gain and efficiency of the proposed antenna is shown in Figure 7. The copolarization gain increases approximately linearly from −1.84 dBi at 2 GHz to a maximum of 7.9 dBi at 9 GHz and then declines in a similar fashion for higher frequencies. The increase in gain is attributed to the increase in effective area of the antenna with frequency. The gain decreases approximately by 4 dB from 9 to 13 GHz because of decreased efficiency. The copolarization gain varies by 5.9 dB within the UWB bandwidth. The efficiency of the antenna decreases from 100% in the range 1–7 GHz to ∼78% from 7 to 13 GHz.

A larger slot size will generally improve the operating bandwidth of the antenna. However, this will be at the expense of the bandwidth of the radiation pattern. Therefore, the first choice here was not to widen the size of the slot to obtain a larger operating bandwidth. Another technique was needed to enhance the antenna's radiation bandwidth and impedance bandwidth. To achieve this, EM coupling needs to be enhanced between the feed and the slot. This necessitates optimizing the physical parameters of the antenna's feed and the slot. The effect of various physical parameters of E-shaped patch and the slot on the performance of the antenna is investigated in the next section.

4. PARAMETRIC STUDY

In this section, a parametric study is undertaken to investigate the physical parameters that influence the performance of the proposed wide-slot antenna.

4.1. Effect of Feed and Slot

To achieve a high level of EM coupling to the feed-line, a large slot size is normally used in the antenna. Therefore, any variation in feed shape or slot shape will change the coupling property; thus, the operating bandwidth is governed by impedance match between the feed shape and the ground-plane slot [2]. On the other hand, an optimum performance can be obtained when the feed and slot shapes are appropriately selected, and the feed occupies an area of about one-third of the slot size.

As mentioned earlier, although a wide-slot antenna provides a wider operating bandwidth, however, its operating bandwidth is limited because of the degradation of the radiation patterns at higher frequencies. In other words, by increasing its frequency of operation, the main beam is tilted away from the broadside direction in *E*-plane because the currents flowing on the edge of the slot will increase the cross-polarization component in the *H*-plane [2].

From the results depicted in Figures 5 and 6, it is obvious that E-shaped patch and feed structure can directly influence the antenna's radiation properties and impedance bandwidth. By changing the position and depth of each protrusion constituting the E-shaped patch, the reflection coefficient changes in the high-frequency region and more impedance bandwidth can be acquired. This is because each protrusion of the E-shaped patch resonates at a high frequency. The consequence of this is that the impedance bandwidth, the radiation bandwidth, and the purity of the current vectors are compromised.

4.2. Effect of Feed Gap t

The feed gap parameter *t* determines the impedance match between the feed-line and the wide-slot antenna. In [2], the feed gap effect on the impedance match is investigated. It is found that by enhancing the coupling between the slot and feed, good impedance matching can be obtained. An optimum operating bandwidth is achievable when the coupling is increased to a certain value. However, if the coupling is increased further more than this value, the impedance matching will deteriorate. This shows that over coupling can degrade the impedance matching

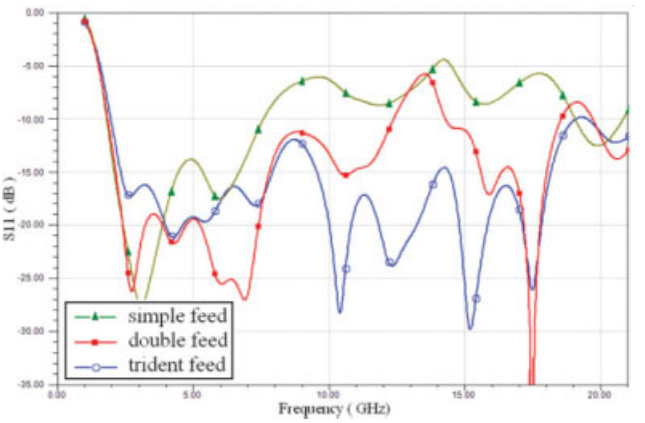

Figure 5 Simulated reflection coefficient of the proposed antenna for various feed-line structures. [Color figure can be viewed in the online issue, which is available at www.interscience.wiley.com]

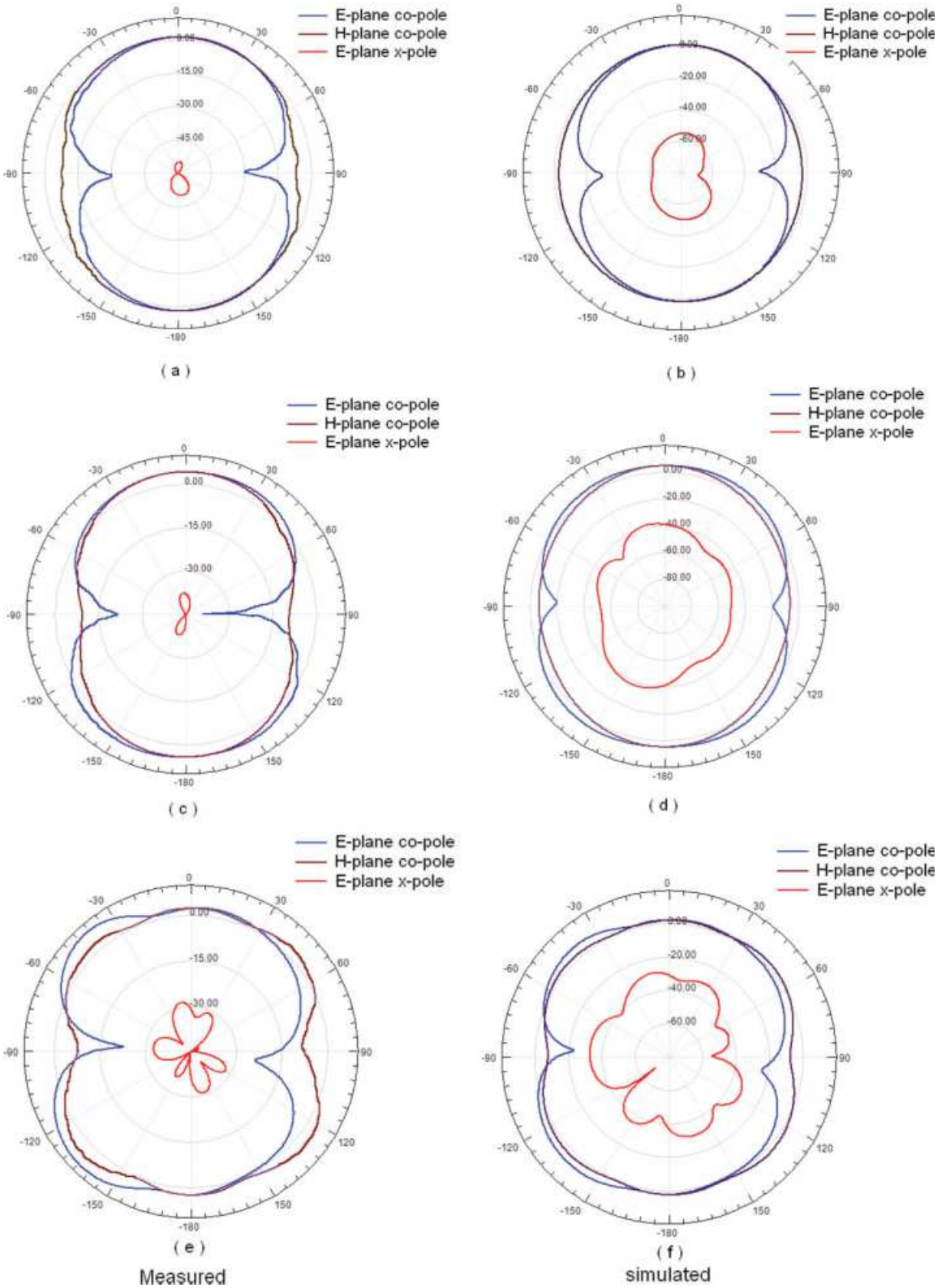

Figure 6 Simulated and measured *E*-plane (*y*–*z*) and *H*-plane (*x*–*z*) radiation patterns of the proposed antenna: (a, b) at 3 GHz, (c, d) at 7 GHz, and (e, f) at 11 GHz. [Color figure can be viewed in the online issue, which is available at www.interscience.wiley.com]

as does under coupling. Figure 8 shows the simulated reflection coefficient of the proposed antenna with feed gaps of 0.5, 1, and 1.5 mm. It can be observed that the frequency corresponding to the lower frequency edge of the bandwidth is clearly independent of the feed gap, but the frequency corresponding to the upper frequency edge is heavily dependent on it. A feed gap value of $t = 1$ mm was selected, as it provides the best wideband response.

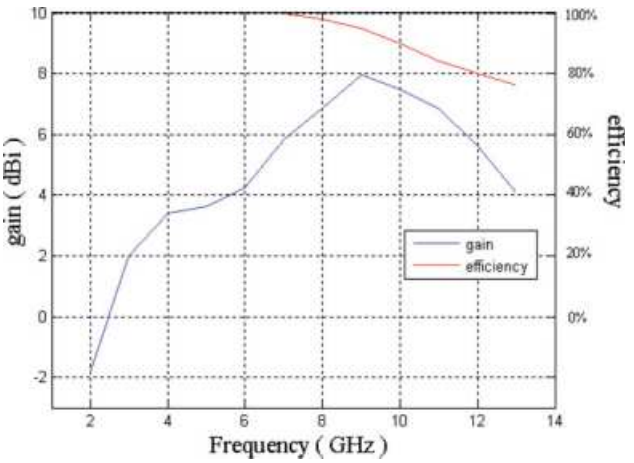

Figure 7 Measured gain and efficiency of the proposed antenna. [Color figure can be viewed in the online issue, which is available at www.interscience.wiley.com]

4.3. *Effect of V*

As was discussed earlier, the antenna's bandwidth can be enhanced by multiplying the feed-line access to the patch. The position of each of the feed branches directly influences the impedance bandwidth. Figure 9 shows the effect on the impedance bandwidth of the proposed antenna by the outer feed-line separation to the trident defined by parameter V. By changing the outer feed-line position to the patch, different modes are excited that cause various current distributions on the E-shaped patch. An optimum feed-line position can be obtained, where the purity of the current distributed on the patch is optimized. In this case, the maximum impedance bandwidth with highest polarization purity is realized when $V = 9.3$ mm.

5. CONCLUSIONS

This article presented the simulation and experimental results of a printed wide-slot antenna. This antenna uses a novel feeding structure in the form of a trident shape to excite a truncated E-shaped patch. This configuration is shown to substantially enhance the antenna's bandwidth and provides high polarization purity. The measured results show good agreement with simulations. The proposed antenna shows a very wide bandwidth of over 163%. In addition to being small in size, the antenna exhibits stable far-field radiation patterns over its operating range, a relatively high gain, and low cross-polarization. Based on these characteristics, the proposed wide-slot antenna can be used for wideband satellite and wireless communication applications.

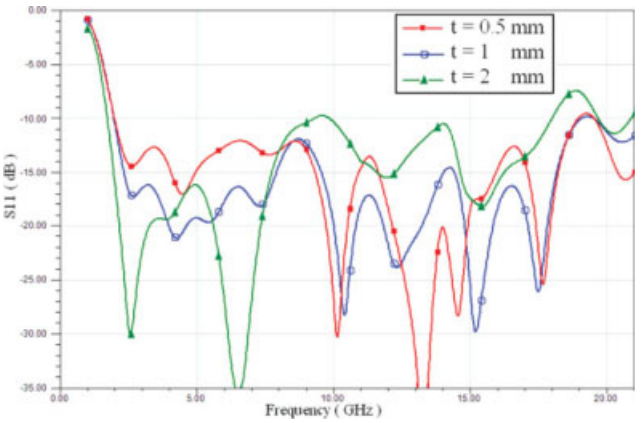

Figure 8 Simulated reflection coefficient of the proposed antenna for various feed gap t values. [Color figure can be viewed in the online issue, which is available at www.interscience.wiley.com]

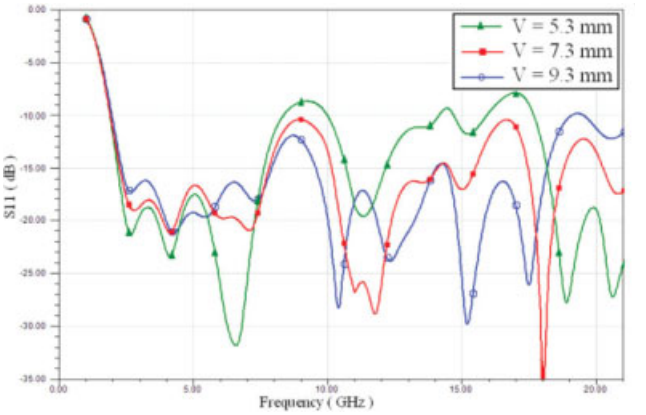

Figure 9 Simulated reflection coefficient of the proposed antenna for various V values. [Color figure can be viewed in the online issue, which is available at www.interscience.wiley.com]

REFERENCES

1. FCC, FCC report and order for part 15 acceptance of ultra wideband (UWB) systems from 3.1–10.6 GHz, Washington, DC, 2002.
2. Y. Liu, K.L. Lau, Q. Xue, and C.H. Chan, Experimental studies of printed wide-slot antenna for wide-band applications, IEEE Antennas Wireless Propag Lett 3 (2004), 273–275.
3. J.Y. Sze and K.L. Wong, Band width enhancement of a microstrip line-fed printed wide-slot antenna, IEEE Trans Antennas Propag 49 (2001), 1020–1024.
4. Y.W. Jang, Experimental study of large bandwidth three-offset microstrip line-fed slot antenna, IEEE Microwave Wireless Compon Lett 11 (2001), 425–426.
5. M.K. Kim, Y.H. Suh, and I. Park, A T-shaped microstrip line-fed wide-slot antenna, Proc IEEE AP-S Int Symp 3 (2000), 1500–1503.
6. Y.W. Jang, Broad band cross-shaped microstrip-fed slot antenna, Electron Lett 36 (2000), 2056–2057.
7. S.W. Qu, C. Ruan, and B.Z. Wang, Bandwidth enhancement of wide-slot antenna fed by CPW and microstrip line, IEEE Antennas Wireless Propag Lett 5 (2006), 15–17.
8. H.D. Chen, Broadband CPW-Fed square slot antennas with a wideband tuning stub, IEEE Trans Antennas Propag 51 (2003), 1982–1985.
9. F. Yang, X.X. Zhang, X. Ye, and Y. Rahmat-Samii, Wide-band E-patched patch antenna for wireless communications, IEEE Trans Antennas Propag 49 (2001), 1094–1100.
10. C.K. Wu and K.L. Wong, Broadband microstrip antenna with directly coupled and gap-coupled parasitic patches, Microwave Opt Technol Lett 22 (1999), 348–349.
11. T. Huynh and K.F. Lee, Single-layer single-patch wideband microstrip antenna, Electron Lett 31 (1995), 1310–1312.
12. Y.X. Guo, C.L. Mak, K.M. Luk, and K.F. Lee, Analysis and design of L-probe proximity fed patch antenna, IEEE Trans Antennas Propag 49 (2001), 145–149.
13. K.L. Wong and Y.F. Lin, Small broadband rectangular microstrip antenna with chip-resistor loading, Electron Lett 33 (1997), 1593–1594.
14. M.A. Gonzalez de Aza, J. Zapata, and J.A. Encinar, Broadband cavity-backed and capacitively probe-fed microstrip patch arrays, IEEE Trans Antennas Propag 48 (2001), 784–789.
15. N. Herscovici, New considerations in the design of microstrip antennas, IEEE Trans Antennas Propag 46 (1998), 807–812.

16. M. Ferrando-Bataller, M. Cabedo-Fabrés, E. Antonino-Daviu, and A. Valero-Nogueira, Overview of planar monopole antennas for UWB applications, Proceedings of the European Conference on Antennas and Propagation, EuCAP 2006 (ESA SP-626), November 2006, pp. 6–10.
17. R.F. Harrington and J.R. Mautz, Theory of characteristic modes for conducting bodies, IEEE Trans Antennas Propag 19 (1971), 622–628.

A NEW TIME DOMAIN SOLUTION FOR THE MULTIPLE DIFFRACTION OF SPHERICAL WAVES BY AN ARRAY OF NONPERFECTLY CONDUCTING WEDGES FOR UWB SIGNALS

Peng Liu and Yunliang Long
Department of Electronics and Communication Engineering, Sun Yat-Sen University, Guangzhou 510275, China; Corresponding author: liupeng5@mail2.sysu.edu.cn

Received 13 July 2009

ABSTRACT: *A time domain (TD) solution for the analysis of multiple diffraction of spherical waves after an array of nonperfectly conducting wedges with different interior angles is presented. The proposed TD solution is based on the representation of the inverse Laplace transform of the corresponding frequency domain solution in closed form, as it is given by a hybrid of the uniform theory of diffraction (UTD)-physic optics (PO) solution. The new formulation, validated with the results from technical literature, does not need to incorporate the TD version of the higher-order diffraction coefficients and allows for the calculation of large number of wedges. It has the major advantage in terms of the mathematical complexity and computation efficiency when compared with other TD solutions.* © 2010 Wiley Periodicals, Inc. Microwave Opt Technol Lett 52: 1006–1008, 2010; Published online in Wiley InterScience (www.interscience.wiley.com). DOI 10.1002/mop.25094

Key words: *radio propagation; time-frequency analysis; ultra-wideband (UWB); uniform theory of diffraction (UTD)*

1. INTRODUCTION

The recent interest in ultra wideband (UWB) system has motivated the propagation analysis of UWB channel characteristics [1–7]. Time domain (TD) solutions with the TD version of the uniform theory of diffraction (UTD) have been used to analyze the scattering or radiation of the UWB pulse from realistic geometry structures. In [8], the TD reflection coefficient for half space was presented. The TD reflection and transmission coefficient through a slab were presented in [3]. For the diffraction phenomena, the TD-UTD solutions, which can be very accurate for early-to-intermediate time, are commonly used. In [6–10], TD single or double diffraction solutions for the canonical objects were obtained. However, in real environment, the transmitted signals usually undergo multiple interactions before it is received. Therefore, to predict the received signals accurately, it is necessary to extend the single or double diffraction solutions to the multiple-diffraction solution. In [4], Qiu derived the channel impulse response of Wolfish-Bertoni's urban propagation configuration in a closed form and quantified the impacts of pulse distortion on a UWB system performance. Karousos and Tzaras have presented a TD-UTD solution for the multiple diffraction caused by a cascade of multimodeled obstacles such as knife-edges and wedges [5]. Such a solution is obtained by incorporating the TD version of the higher-order diffraction coefficients which provided accurate results while at the same time increasing both the mathematical complexity and computation time of the formulation. In this work, a new TD solution in terms of the TD-UTD coefficients for the multiple diffraction of spherical waves by an array of nonperfectly conducting wedges with different interior angles is presented. Such solution does not need to incorporate the TD representation of the higher-order diffraction coefficients because of a recursive relation and allows for the calculation of large number of wedges, thus providing an easier and faster method without any compromise on the accuracy of the results. The TD solution is valid for wedges with the same height, which is relative to the base station antenna height and separated by a constant distance.

2. PROPAGATION ENVIRONMENT

The propagation environment considered in this work is shown in Figure 1, where an array of finitely conducting wedges with different interior angles has been taken into account. The wedges are assumed to have the same height (relative to the base station antenna height, H) and separated by a constant distance, w. The transmitter is at an arbitrary height and is located at a certain distance d from the array of structure. The incident spherical wave impinges on the first wedge with an angle α. We will first borrow some well-known frequency domain results from radio propagation literature. Then, the inverse Laplace transform is applied to obtain the TD solution.

3. FREQUENCY DOMAIN MODEL

For the scenario similar to Figure 1, a hybrid of UTD-PO formulation is presented in [11] for the analysis of multiple diffraction caused by an array of perfectly conducting wedges with the same interior angle. The solution does not need to incorporate the slope or higher-order diffraction coefficients because of a recursive relation in which only single diffractions are involved in the calculation, thus significantly reducing the mathematical complexity and computation time of the formulation. Regarding the above, for $N \geq 1$, the electric field at the reference point in Figure 1 can be expressed as:

i. Base station antenna above or level with the average height of the wedges ($H = 0$):

$$E_N(\omega) = \frac{1}{N}\sum_{m=0}^{N-1} E_m(\omega)\left[\frac{s_0}{s_{N-m}} e^{-jk(s_N - s_m)} + \sqrt{\frac{s_0}{(N-m)w[s_0+(N-m)w]}} D(\gamma_{m+1}, L_m) e^{-jk(N-m)w}\right], \quad (1)$$

where

$$E_0(\omega) = \frac{E^i e^{-jks_0}}{s_0} \quad (2)$$

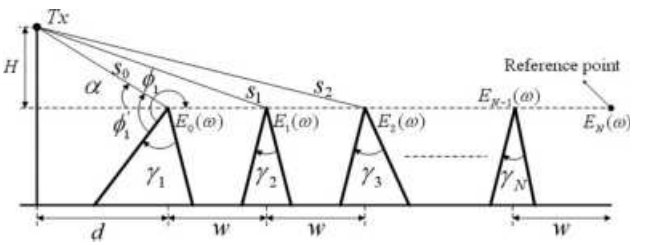

Figure 1 Scheme of the considered pulse propagation environment